

Regulation of Epithelial Cell Tight Junctions by Protease-Activated Receptor 2

Shuhei ENJOJI¹⁾, Takashi OHAMA¹⁾ and Koichi SATO^{1)*}

¹⁾Laboratory of Veterinary Pharmacology, Joint Faculty of Veterinary Medicine, Yamaguchi University, 1677-1 Yoshida, Yamaguchi 753-8515, Japan

(Received 8 April 2014/Accepted 13 May 2014/Published online in J-STAGE 30 May 2014)

ABSTRACT. A layer of epithelial cells prevents the invasion of bacteria and the entry of foreign substances into the underlying tissue. The disruption of epithelial tight junctions initiates and exacerbates inflammation. However, the precise mechanism underlying the disruption of the epithelial tight junction remains unclear. The activation of protease-activated receptor 2 (PAR2) by serine proteases produced by some bacteria and mast cells contributes to inflammation in many tissues. In the present study, we tested the hypothesis that PAR2 activation affects the structure and function of tight junctions in Madin-Darby canine kidney (MDCK) cells. Although the application of a PAR2-activating peptide, PAR2-AP, from the apical side of MDCK cells failed to modify the transepithelial resistance (TER), its application from the basal side markedly suppressed the TER. In 3-dimensional cultures of MDCK cells expressing the mCherry-tagged PAR2, a lateral localization of PAR2 was observed. The application of PAR2-AP from the basal side changed the localization of the tight junctional protein, zonula occludin-1. Furthermore, PAR2-AP induced the phosphorylation of p38 MAP kinase. A p38 MAP kinase inhibitor, SB202190, inhibited PAR2-AP-induced changes in TER. Our results suggest that the activation of PAR2 leads to the disruption of tight junctions and increases the barrier permeability through the activation of p38 MAPK, which may cause the initiation and exacerbation of inflammation.

KEY WORDS: epithelium, protease activated receptor, tight junction

doi: 10.1292/jvms.14-0191; *J. Vet. Med. Sci.* 76(9): 1225–1229, 2014

A layer of epithelial cells forms a barrier that covers the surface of tissues, such as skin, intestine and lung. Assisted by the formation of the apical junction complex, containing tight junctions, adherence junctions and desmosomes, the epithelial cell layer serves as a barrier that prevents bacterial entry, while allowing efficient transport of nutrients across the membrane.

Tight junctions are essential for the formation of an epithelial barrier [14]. Tight junctions contain occludin and claudin, both of which form the homophilic adhesion at the extracellular region. Zonula occludin-1 (ZO-1) binds to the intracellular region of occludin and claudin and functions as a scaffold protein along with actin filaments to provide stability to adhesion [5]. In epithelial cells, the tight junction is involved in the establishment of cell polarity between the apical and basolateral sides [4].

Changes in the expression and function of tight junction proteins result in the hyperpermeability of epithelial cells and lead to many diseases, including renal disorders and rheumatoid arthritis [6]. In gastro-intestinal epithelial cells, disruption of tight junctions permits the invasion of bacteria and exacerbates inflammation. Under inflammatory conditions, the epithelial tight junctions are disrupted by stimulations from the apical and basal sides [1]. However, the

precise mechanisms by which tight junctions are disrupted remain incompletely understood.

The protease-activated receptor 2 (PAR2), a member of G-protein coupled receptors, is expressed in many tissues, including the gut, pancreas, liver and kidney, and contributes to inflammation. PAR2 is a tethered ligand receptor, which can be proteolytically activated by trypsin, mast cell tryptase and the coagulation factors VIIa and Xa [8]. Additionally, some bacterial proteases activate PAR2 in gastro-intestinal epithelial cells, leading to the production of inflammatory cytokines [2]. Consistent with this finding, inflammatory reactions are suppressed in PAR2 knockout (PAR2-KO) mice [17]. However, the precise mechanism by which PAR2 promotes inflammation is unknown. Therefore, we tested the hypothesis that PAR2 activation disrupts tight junctions and inhibits their function.

MATERIALS AND METHODS

Cell culture: Madin-Darby canine kidney (MDCK) epithelial cells were grown in Dulbecco's modified Eagle's medium supplemented with 10% FBS and 1× antibiotic-antimycotic solution (Life Technologies Gibco, Carlsbad, CA, U.S.A.).

Antibodies and reagents: The antibodies used for this study included E-cadherin (#610181; BD Bioscience, Franklin Lakes, NJ, U.S.A.), occludin (sc-5562; Santa Cruz Biotechnology, Dallas, TX, U.S.A.), phospho-ERK p42/p44 (#9101), phospho-p38 MAPK Thr180/182 (#9216) phospho-Ser473 Akt1 (#07-310; all from Cell Signaling Technology, Danvers, MA, U.S.A.), α -tubulin (RB-9281-P0; Thermo Scientific, Waltham, MA, U.S.A.) and ZO-1 (#339100; Invitrogen, Carlsbad, CA, U.S.A.). FR180204, SB202190 and

*CORRESPONDENCE TO: SATO, K., Laboratory of Veterinary Pharmacology, Joint Faculty of Veterinary Medicine Yamaguchi University, 1677-1 Yoshida, Yamaguchi 753-8515, Japan.

e-mail: k-sato@yamaguchi-u.ac.jp

©2014 The Japanese Society of Veterinary Science

This is an open-access article distributed under the terms of the Creative Commons Attribution Non-Commercial No Derivatives (by-nc-nd) License <<http://creativecommons.org/licenses/by-nc-nd/3.0/>>.

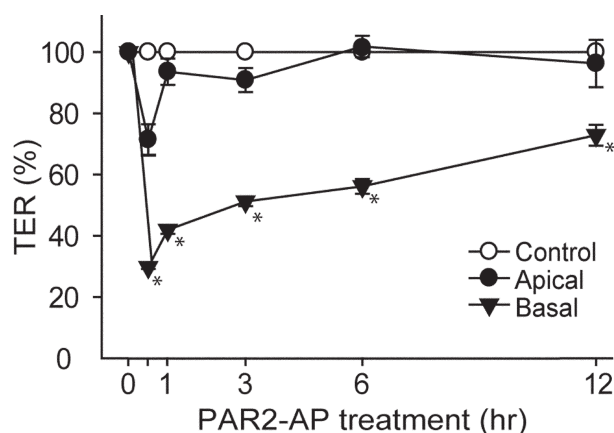


Fig. 1. Application of PAR2-activating peptide (PAR2-AP) from the basal side of Madin-Darby canine kidney (MDCK) cells decreases transepithelial electrical resistance (TER). TER across MDCK cells was measured following stimulation without (Control) or with PAR2-AP (100 μ M) from the apical side (Apical) or the basal side (Basal) for indicated periods. TER of MDCK cells at 0 hr was considered 100%. * P <0.05 vs. Control. N=3.

wortmannin were purchased from Sigma-Aldrich (St. Louis, MO, U.S.A.). The SLIGRL-NH2 PAR2-activating peptide (PAR2-AP) was purchased from Abgent (San Diego, CA, U.S.A.), and SP600125 was purchased from Cayman (Ann Arbor, MI, U.S.A.). These reagents were dissolved with dimethyl sulfoxide except for PAR2-AP, which was dissolved with distilled water. All other chemicals were purchased from Wako Pharmaceuticals (Osaka, Japan).

Generation of MDCK cells stably expressing PAR2-mCherry: The lentivirus plasmid used for expressing PAR2-mCherry has been described elsewhere [9]. To produce the lentivirus plasmids, 3 μ g of pLVmCC human PAR2 plasmid, 2.3 μ g of a packaging plasmid (psPAX2) and 1.3 μ g of a coat-protein plasmid-harboring vesicular stomatitis virus G protein (pMD2.G) were transfected into Lenti-X 293T cells cultured in 60-mm dishes. Forty-eight hours after transfection, the viral supernatants were collected, filtered through a 0.22- μ m filter and used to infect MDCK cells (for 8 hr) to generate mCherry-PAR2 MDCK cells.

Measurement of transepithelial electrical resistance (TER): The TER across MDCK cells cultured in 24-well transwell plate (pore size 0.4 μ m, BD Falcon, San Jose, CA, U.S.A.) was measured using EVOM2 epithelial volt-ohmmeter (WPI, Sarasota, FL, U.S.A.) equipped with an STX2 electrode. The value obtained from the blank sample was subtracted from that obtained from the test sample to obtain the net resistance, which was multiplied by the area of the membrane to yield the resistance in area-corrected units (Ω -cm²). The change in electrical resistance was estimated as the percentage baseline resistance. Before the measurement of TER, the cells were adapted to room temperature for less than 5 min.

Three-dimensional culture of MDCK cells: For the 3-dimensional culture, a 12-mm coverglass, placed in 1

well of a 24-well plastic plate, was coated with 50 μ l of Matrigel Matrix (BD Biosciences, San Jose, CA, U.S.A.) for 15 min. Following this, 1 ml of MDCK cell suspension (2×10^4 cells/ml) containing 20 μ l of Matrigel Matrix was added to the coated coverglass, and the cells were cultured for 3 days to form cysts.

Immunofluorescence microscopy: mCherry-PAR2 MDCK cells (7×10^5) were cultured in a 12-well type transwell insert (Corning Incorporation, New York, NY U.S.A.) for 4 days. The cells were then fixed with a 1:1 mixture of methanol and acetone for 10 min at -20°C . For imaging, the cysts were fixed with 4% paraformaldehyde in phosphate-buffered saline (PBS) for 30 min at room temperature. Cells and cysts were washed with PBS containing 0.05% Tween 20 (PBS-T) and then blocked with PBS-T containing 3% skim milk for 30 min. After incubation with primary antibodies (1:400 in PBS-T) overnight at 4°C , the cells were incubated with Alexa Fluor 488-conjugated secondary antibodies (1:2,000 in PBS-T) for 1 hr at room temperature. The immunofluorescently labeled cells were examined, and images were acquired with a LSM510 confocal microscope (Carl Zeiss, Inc., Thornwood, CA, U.S.A.). To stain the actin filaments, cysts were incubated with DY-649-Phalloidin (1:2,000 dilution; Dynamics GmbH, Jena, Germany) for 60 min.

Western blotting: Cells were lysed using a buffer containing 50 mM Tris-HCl (pH 8.0), 5 mM EDTA (pH 8.0), 5 mM EGTA, 1% Triton X100, 1 mM Na₃VO₄, 20 mM sodium pyrophosphate and Roche's complete protease inhibitor cocktail. Proteins present in the lysate were separated by sodium dodecyl sulfate-polyacrylamide gel electrophoresis and electrophoretically transferred onto a polyvinylidene difluoride membrane (Bio-Rad, Hercules, CA, U.S.A.). Following this, the membranes were blocked with 0.5% skim milk for 1 hr, incubated with primary antibodies, washed and incubated with desired secondary antibodies. After washing the membrane, the specific immunocomplexes formed were detected with ECL Western Blotting Detection System (GE healthcare, Little Chalfont, UK) or ECL Pro (Perkin Elmer, Waltham, MA, U.S.A.) and visualized using the LAS-3000 imager (Fujifilm, Tokyo, Japan).

Statistical analysis: Results of the statistical analysis are expressed as mean \pm standard error of the mean (SEM) values. Paired or unpaired Student's *t*-tests were used for comparisons between the 2 groups. One-way analysis of variance (ANOVA) followed by Student-Newman-Keuls test was used for comparisons between more than 3 groups. For all analyses, P <0.05 indicated statistical significance.

RESULTS

We examined the effect of PAR2 stimulation on TER, a major marker of tight junction formation, in MDCK cells. A PAR2-activating peptide (PAR2-AP, 100 μ M) was applied onto the cell culture insert (apical side of MDCK) or into the well (basal side of MDCK). Although the stimulation with PAR2 from the apical side did not alter the TER, the stimulation from the basal side significantly suppressed the TER after 30 min (Fig. 1). This result suggested that PAR2

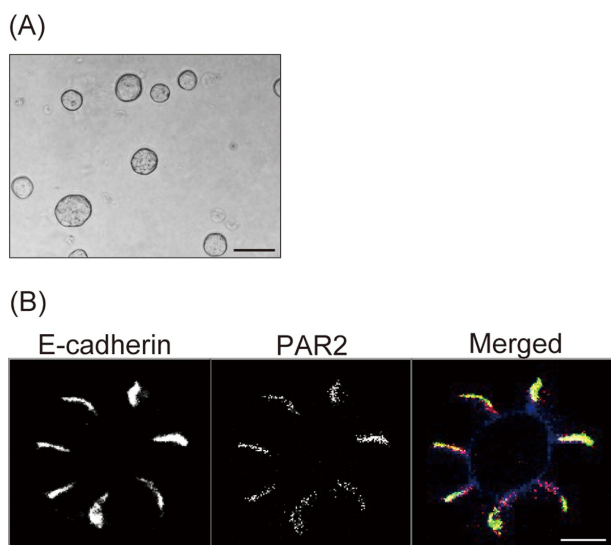


Fig. 2. PAR2 localizes to the basolateral side of MDCK cystic cells. The mCherry-PAR2 MDCK cells were cultured in Matrigel to form cysts. Phase contrast image of cysts (A) and confocal fluorescence microscopy images of E-cadherin (left panel), mCherry-PAR2 (middle panel), and merged image of E-cadherin (green), mCherry-PAR2 (red) and actin (blue) (right panel) (B). Representative images from 3 independent experiments are shown. Scale bars; 800 μm (A) and 50 μm (B).

was localized to the basal side of MDCK cells.

Next, we examined the localization of PAR2 in 3-dimensional cultures of the polyclonal mCherry-PAR2 MDCK cells. After 3 days of culture in Matrigel matrix, these cells formed a spherical cyst (Fig. 2A). Confocal microscopy analysis revealed the colocalization of mCherry-PAR2 with E-cadherin (lateral marker), but not with actin (apical marker) (Fig. 2B). This result suggested that PAR2 was specifically localized to the lateral side of epithelial cells.

We next examined the effect of PAR2 activation on the localization of the tight junctional proteins, occludin and ZO-1. MDCK cells cultured in a transwell insert were treated with 100 μM PAR2-AP from the apical or basal sides. In the absence of PAR2-AP, both occludin (Fig. 3A) and ZO-1 (Fig. 3B) localized to the lateral side of MDCK cells. Treatment with PAR2-AP for 30 min from the basal side, but not from apical side, altered the ZO-1 localization from the membrane to the cytoplasm. The localization of occludin was unaffected by the addition of PAR2-AP from either the apical side or the basal side. These results suggested that PAR2 was localized to the basolateral side and that the treatment of the cells with PAR2-AP from the apical side failed to activate PAR2 because tight junctions interfered with the passing of PAR2-AP.

We next investigated the effects of PAR2-AP on the phosphorylation of p38 MAPK, ERK1/2 and Akt by western blotting. The stimulation of the MDCK cells with PAR2-AP (100 μM) from the basal side significantly increased the phosphorylation of p38 MAPK, ERK1/2 and Akt within

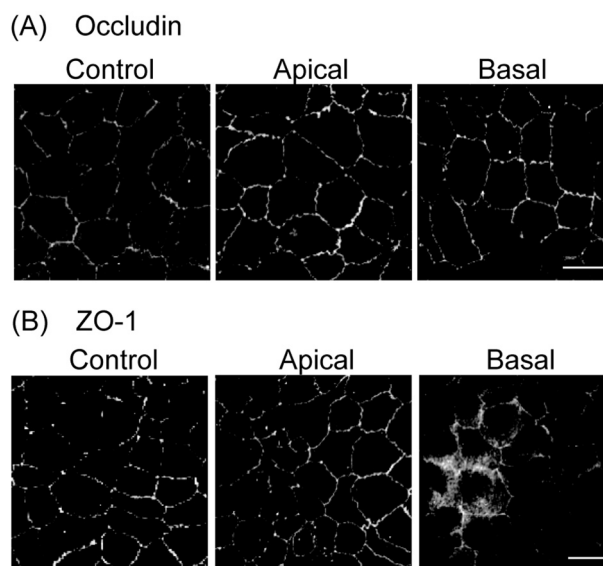


Fig. 3. PAR2 stimulation changes the localization of ZO-1 proteins in MDCK cells. Localization of occludin (A) and ZO-1 (B) in MDCK cells, before (Control) and after the application of PAR2-AP (100 μM) for 30 min from the apical side (Apical) or the basal side (Basal), was analyzed by confocal microscopy. Representative images from 3 independent experiments are shown. Scale bar, 50 μm .

10 min (Fig. 4). Pretreatment of the cells with FR1802904 (30 μM , an ERK1/2 inhibitor), SP600125 (10 μM , a JNK inhibitor) and wortmannin (100 μM , a PI3K-Akt inhibitor) for 30 min had no effect on the PAR2-AP-induced changes in TER. None of the inhibitors evaluated had any significant effect on the resting TER (data not shown). In contrast, pretreatment of the cells with 10 μM SB202190, a p38 MAPK inhibitor, significantly reversed the effect of PAR2-AP on TER (Fig. 5). These results suggested that PAR2 stimulation suppressed TER through a mechanism that involved p38 MAPK activation.

DISCUSSION

Epithelial tight junctions are critical for preventing the invasion of bacteria and the entry of harmful foreign materials [14]. The disruption of tight junctions leads to infection and inflammation. The results suggest that the activation of PAR2 from the basolateral side of epithelial cells leads to the disruption of tight junctions in MDCK epithelial cells.

PAR2 is activated by mast cell tryptase as well as coagulation factors VIIa and Xa [8]. Therefore, mast cell degranulation and vascular hyperpermeability could result in the activation of PAR2, leading to the disruption of tight junctions. Consistent with this finding, the inflammatory agents produced from mast cells following the recognition of a food allergy protein can disrupt intestinal epithelial tight junctions from the basal side [19]. Although PAR2-AP treatment from the apical side failed to activate PAR2 in MDCK

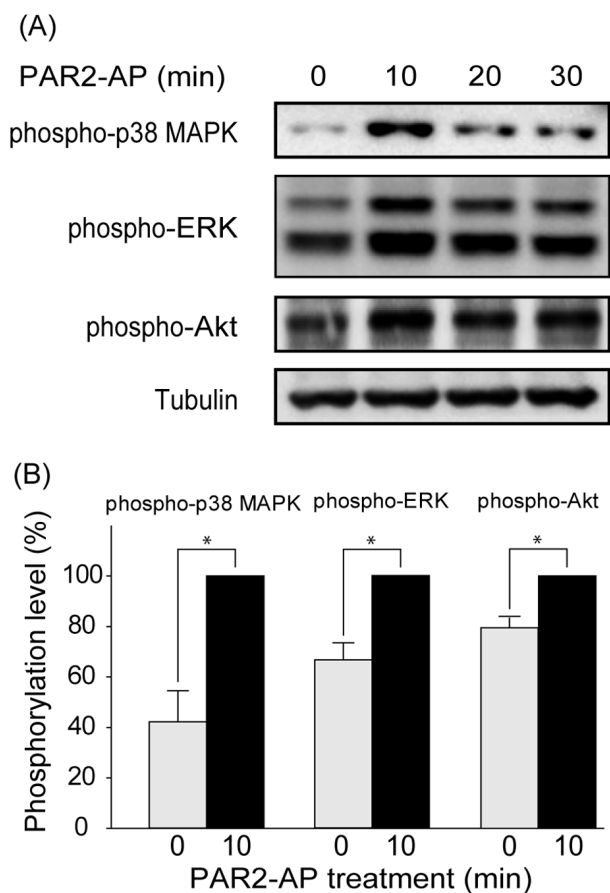


Fig. 4. PAR2 stimulation increases the phosphorylation of p38 MAPK, ERK1/2 and Akt. MDCK cells were treated with PAR2-AP (100 μ M) from the basal side for indicated periods. Phosphorylated proteins and tubulin were quantified by western blotting. Representative images from 3 experiments are shown (A). Band density was normalized to the phosphorylation level at 10 min after PAR2 stimulation in the same series of experiments (B). The results are expressed as mean \pm SEM of 3 independent experiments. * P <0.05.

cells, it is possible that under inflammatory conditions, PAR2-activators from the apical side of the epithelial cells can activate PAR2 owing to the epithelial hyperpermeability and the invasion of bacteria and exotoxins [7]. It has been reported that a protease produced by a member of the genus *Helicobacter* activates PAR2, leading to the exacerbation of inflammation [17].

Our study showed that PAR2 was localized to the lateral side of MDCK cells. It has been reported that PAR2 localizes to the apical side of human cornea epithelial cells and to the basal side of human esophageal epithelial cells [10, 15]. These studies used anti-PAR2 antibodies and PAR2-agonists labeled with fluorescent protein to examine the localization of PAR2. In contrast, we used mCherry-tagged PAR2 in our experiments. It is likely that non-specific binding of the PAR2 antibodies and agonists contributed to the reported differences in the localization of PAR2. Alternatively, the differences in the localization of PAR2 may be attributed to

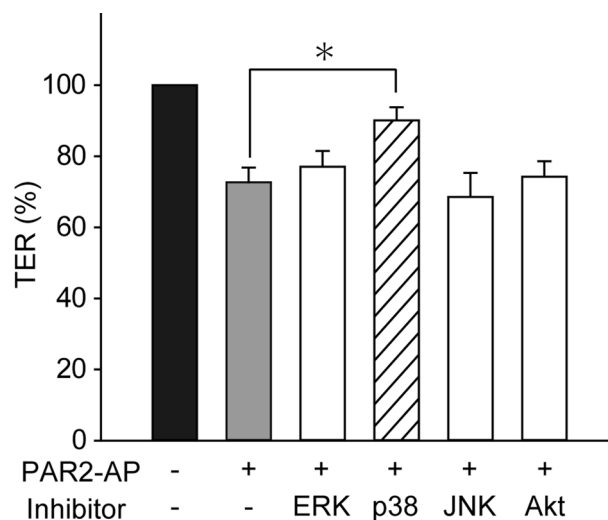


Fig. 5. The p38 MAPK inhibitor blocks the inhibitory effect of PAR2-AP on TER. Cells were treated with inhibitors of ERK1/2 (FR1802904, 30 μ M), p38 MAPK (SB202190, 10 μ M), JNK (SP600125, 10 μ M) and PI3K-Akt (wortmannin, 100 μ M) for 30 min before the application of PAR2-AP (100 μ M). The TER of MDCK cells was measured in the presence and absence of PAR2-AP for 30 min. TER immediately before the application of PAR2-AP was considered 100%. * P <0.05 vs. without PAR2-AP application. N=8.

differences in the posttranslational modification of PAR2, such as glycosylation [3], which changes protein folding and alters localization [18].

We observed a change in the localization of ZO-1, but not in that of occludin, from the cell membrane to the cytoplasm following PAR2 stimulation. We found that PAR2 activation induced the phosphorylation of ERK1/2, p38 MAPK and Akt in MDCK cells. However, only p38 MAPK contributed to changes in TER downstream of PAR2 activation. Our results are consistent with that of a previous study, which showed that the activation of p38 MAPK led to reduced ZO-1 expression and the dissociation of ZO-1 from cell membrane [13]. Unfortunately, molecular mechanisms underlying activated p38 MAPK-induced tight junction disruption remain to be elucidated. Several studies have suggested that tight junctions can be disrupted by various stimuli through the p38 MAPK pathway [11, 13, 16]. However, further experiments are required to elucidate the exact mechanism by which p38 MAPK disrupts tight junctions. We found that the PAR2-AP-induced changes in TER reached a peak within 30 min of stimulation. This result suggested that the PAR2-AP-induced reduction in TER was caused by the changes in tight junction structure/function and not by the reduced protein expression. It has been reported that ZO-1 phosphorylation induces hyperpermeability in epithelial cells [12]. Together with these reports, our results suggest that p38 MAPK or a downstream kinase of p38 MAPK may phosphorylate ZO-1, thereby causing hyperpermeability and a reduction in TER.

We have shown that PAR2 localized to the basolateral

side of MDCK cells and tight junctions denied permeability to the PAR2 activator when it was applied from the apical side. We also showed that PAR2 activator from the basal side induced the phosphorylation of p38 MAPK, which led to hyperpermeability and a change in ZO-1 localization. These results suggest that mast cell degranulation and increased vessel permeability, as observed under inflammatory and allergic conditions, worsen inflammation by activating PAR2 in epithelial cells. Therefore, our results suggest that PAR2 inhibitors may serve as useful anti-inflammatory agents.

ACKNOWLEDGMENTS. This work was partly supported by a Grant-in-Aid for Scientific Research from the Japanese Ministry of Education, Culture, Sports, Science and Technology. The funding source had no role in the study design; collection, analysis or interpretation of data; in the writing of the manuscript; or the decision to submit the manuscript for publication.

REFERENCES

1. Bruewer, M., Luegering, A., Kucharzik, T., Parkos, C. A., Madara, J. L., Hopkins, A. M. and Nusrat, A. 2003. Proinflammatory cytokines disrupt epithelial barrier function by apoptosis-independent mechanisms. *J. Immunol.* **171**: 6164–6172. [[Medline](#)] [[CrossRef](#)]
2. Cenac, N., Coelho, A. M., Nguyen, C., Compton, S., Andrade-Gordon, P., MacNaughton, W. K., Wallace, J. L., Hollenberg, M. D., Bunnett, N. W., Garcia-Villar, R., Bueno, L. and Vergnolle, N. 2002. Induction of intestinal inflammation in mouse by activation of proteinase-activated receptor-2. *Am. J. Pathol.* **161**: 1903–1915. [[Medline](#)] [[CrossRef](#)]
3. Compton, S. J., Renaux, B., Wijesuriya, S. J. and Hollenberg, M. D. 2001. Glycosylation and the activation of proteinase-activated receptor 2 (PAR2) by human mast cell tryptase. *Br. J. Pharmacol.* **134**: 705–718. [[Medline](#)] [[CrossRef](#)]
4. Fletcher, G. C., Lucas, E. P., Brain, R., Tournier, A. and Thompson, B. J. 2012. Positive feedback and mutual antagonism combine to polarize Crumbs in the *Drosophila* follicle cell epithelium. *Curr. Biol.* **22**: 1116–1122. [[Medline](#)] [[CrossRef](#)]
5. Furuse, M., Itoh, M., Hirase, T., Nagafuchi, A., Yonemura, S. and Tsukita, S. 1994. Direct association of occludin with ZO-1 and its possible involvement in the localization of occludin at tight junctions. *J. Cell Biol.* **127**: 1617–1626. [[Medline](#)] [[CrossRef](#)]
6. Harhaj, N. S. and Antonetti, D. A. 2004. Regulation of tight junctions and loss of barrier function in pathophysiology. *Int. J. Biochem. Cell Biol.* **36**: 1206–1237. [[Medline](#)] [[CrossRef](#)]
7. Kajikawa, H., Yoshida, N., Katada, K., Hirayama, F., Handa, O., Kokura, S., Naito, Y. and Yoshikawa, T. 2007. Helicobacter pylori activates gastric epithelial cells to produce interleukin-8 via protease-activated receptor 2. *Digestion* **76**: 248–255. [[Medline](#)] [[CrossRef](#)]
8. Kawabata, A. and Kuroda, R. 2000. Protease-activated receptor (PAR), a novel family of G protein-coupled seven transmembrane domain receptors: activation mechanisms and physiological roles. *Jpn. J. Pharmacol.* **82**: 171–174. [[Medline](#)] [[CrossRef](#)]
9. Komatsu, H., Enjouji, S., Ito, A., Ohama, T. and Sato, K. 2013. Prostaglandin E₂ inhibits proteinase-activated receptor 2-signal transduction through regulation of receptor internalization. *J. Vet. Med. Sci.* **75**: 255–261. [[Medline](#)] [[CrossRef](#)]
10. Lang, R., Song, P. I., Legat, F. J., Lavker, R. M., Harten, B., Kalden, H., Grady, E. F., Bunnett, N. W., Armstrong, C. A. and Ansel, J. C. 2003. Human corneal epithelial cells express functional PAR-1 and PAR-2. *Invest. Ophthalmol. Vis. Sci.* **44**: 99–105. [[Medline](#)] [[CrossRef](#)]
11. Lui, W. Y., Wong, C. H., Mruk, D. D. and Cheng, C. Y. 2003. TGF-beta3 regulates the blood-testis barrier dynamics via the p38 mitogen activated protein (MAP) kinase pathway: an *in vivo* study. *Endocrinology* **144**: 1139–1142. [[Medline](#)] [[CrossRef](#)]
12. Ohtake, K., Maeno, T., Ueda, H., Ogihara, M., Natsume, H. and Morimoto, Y. 2003. Poly-L-arginine enhances paracellular permeability via serine/threonine phosphorylation of ZO-1 and tyrosine dephosphorylation of occludin in rabbit nasal epithelium. *Pharm. Res.* **20**: 1838–1845. [[Medline](#)] [[CrossRef](#)]
13. Peerapen, P. and Thongboonkerd, V. 2013. p38 MAPK mediates calcium oxalate crystal-induced tight junction disruption in distal renal tubular epithelial cells. *Sci. Rep.* **3**: 1041. [[Medline](#)] [[CrossRef](#)]
14. Schneeberger, E. E. and Lynch, R. D. 2004. The tight junction: a multifunctional complex. *Am. J. Physiol. Cell Physiol.* **286**: C1213–C1228. [[Medline](#)] [[CrossRef](#)]
15. Shan, J., Oshima, T., Chen, X., Fukui, H., Watari, J. and Miwa, H. 2012. Trypsin impaired epithelial barrier function and induced IL-8 secretion through basolateral PAR-2: a lesson from a stratified squamous epithelial model. *Am. J. Physiol. Gastrointest. Liver Physiol.* **303**: G1105–G1112. [[Medline](#)] [[CrossRef](#)]
16. Shirasawa, M., Sonoda, S., Terasaki, H., Arimura, N., Otsuka, H., Yamashita, T., Uchino, E., Hisatomi, T., Ishibashi, T. and Sakamoto, T. 2013. TNF- α disrupts morphologic and functional barrier properties of polarized retinal pigment epithelium. *Exp. Eye Res.* **110**: 59–69. [[Medline](#)] [[CrossRef](#)]
17. Velin, D., Narayan, S., Bernasconi, E., Busso, N., Ramelli, G., Maillard, M. H., Bachmann, D., Pythoud, C., Bouzourene, H., Michetti, P. and So, A. 2011. PAR2 promotes vaccine-induced protection against Helicobacter infection in mice. *Gastroenterology* **141**: 1273–1282, 1282.e1271. [[Medline](#)] [[CrossRef](#)]
18. Weng, T. Y., Chiu, W. T., Liu, H. S., Cheng, H. C., Shen, M. R., Mount, D. B. and Chou, C. Y. 2013. Glycosylation regulates the function and membrane localization of KCC4. *Biochim. Biophys. Acta* **1833**: 1133–1146. [[Medline](#)] [[CrossRef](#)]
19. Yu, L. C. 2012. Intestinal epithelial barrier dysfunction in food hypersensitivity. *J. Allergy (Cairo)* **2012**: 596081. [[Medline](#)]